International Commission on Illumination
Commission Internationale de l'Eclairage
Internationale Beleuchtungskommission

# OP50

# USING RADIANCE TO ESTIMATE TRANSMITTED SOLAR RADIATION ENERGY FOR THIN PERFORATED SCREENS

**Doris Abigail Chi Pool et al.**

DOI 10.25039/x46.2019.OP50

from

CIE x046:2019

Proceedings
of the
29th CIE SESSION
Washington D.C., USA, June 14 – 22, 2019

(DOI 10.25039/x46.2019)

The paper has been presented at the 29th CIE Session, Washington D.C., USA, June 14-22, 2019. It has not been peer-reviewed by CIE.



CIE Central Bureau
Babenbergerstrasse 9
A-1010 Vienna
Austria
Tel.: +43 1 714 3187
e-mail: ciecb@cie.co.at
www.cie.co.at

# USING RADIANCE TO ESTIMATE TRANSMITTED SOLAR RADIATION ENERGY FOR THIN PERFORATED SCREENS

**Chi, D.A.**[1], Brembilla, E.[2]
[1] Department of Architecture, Universidad de las Americas Puebla, MEXICO, [2] School of Architecture, Building and Civil Engineering, Loughborough University, UNITED KINGDOM

doris.chi@udlap.mx

DOI 10.25039/x46.2019.OP50

## Abstract

Design of shading systems is essential, since they plays an important role in the modulation of daylight and solar gains. Yet, current simulation tools are not capable of providing accurate results for both daylighting and energy performance simultaneously, especially when complex geometries are present. This work investigates whether shading coefficients (SC) can be applied to evaluate the performance of thin screens, and it compares the results to those obtained through other methods, such as the use of a fixed transmittance value over the whole year. Results showed that hourly SC can take into account the variability of total transmitted solar radiation throughout the year. As a result, the cooling energy reached reductions of up to 22 % in comparison to the use of a fixed transmittance value. SC also enabled the assessment of inter-reflections within the PS-glazing system, especially those resulted from varying the distance between the PS and glazing.

*Keywords*: Radiance, solar radiation energy, perforated screen, shading coefficient.

## 1 Introduction

Building solar design can take many different forms to answer different goals, ranging from purely aesthetic criteria to the careful modulation of daylight and solar penetration (Bellia et al., 2013). Recent developments in computer-aided design programs enabled architects to explore complex geometries for building envelopes. Design methodologies and tools to accurately and efficiently simulate the daylight and energy performance of complex shading systems are becoming essential, since they can greatly influence design decisions. Furthermore, for whole-building assessments, Climate-based daylight simulations should be run in synergy with energy calculations to find a balance between achieving well-daylit spaces and limiting solar gains.

Yet, current simulation tools are not capable of providing accurate results for both daylighting and energy performance simultaneously, especially when complex geometries are present (Kim and Park, 2011). Radiance is a validated backward ray-tracer capable of simulating complex geometries (Ward, 1992). It has been shown that rtrace-based methods can accurately represent the geometrical feature/pattern of light through a perforated screen (PS). Conversely, Radiance 'phased' methods that use BSDF materials can lose the definition of the fenestration system's shape completely (Brembilla et al., 2017). EnergyPlus has been validated thoroughly for assessing the energy performance of conventional building systems and is one of the most accessible professional energy simulation engines available. However, at this moment there is no way to represent complex geometries within its energy calculation engine. Moreover, EnergyPlus uses a simplified method to account for light redirection, once again not appropriate for complex spaces and facades (Ramos and Ghisi, 2010).

To overcome the simulation tools' limitations, few methods to integrate various software packages were proposed. For thick shading systems, one method consisted of sharing annual shading schedules between Radiance and EnergyPlus (Azadeh, 2011): shading coefficients (SC) were generated with Radiance to analyze the dual performance of three-dimensional complex shading systems that have the capability to both shade and redirect daylight into interior space. Similarly, flat screens characterized by different perforation ratios remain a challenging simulation task for EnergyPlus, but so far only a limited number of studies addressed this problem. Since shadows are projected in parallel, it is common to simplify the

screen energy modelling by assuming a transmittance equal to their perforation ratio. However, previous studies showed that the light inter-reflections between the inner face of PS and the glazing systems must not be disregarded (Chi et al., 2018).

### 1.1 Objective

This work investigates whether SC can be applied to evaluate the performance of thin screens, and it compares the results to those obtained through other methods, such as the use of a fixed transmittance value over the whole year and the use of Bidirectional Scattering Distribution Functions (BSDF). The objective is to analyze if annual transparency schedules can characterize the variability of transmitted solar radiation for different complex shading screens when calculating solar loads and annual energy consumption in EnergyPlus. Furthermore, this study compares the effects of varying the distance within the system (PS + glazing) with illuminance and SC values for different seasons throughout the year. In brief, this work analyses the direct and indirect light transmission through thin PS modelled with different strategies and their impact in luminous environment and energy consumption in office buildings.

## 2 Methodology

### 2.1 Case study and PS modelling

The case study is an office space measuring 7 m x 7 m and 3 m in height. It has a fully glazed South façade with a 78.1 % visible transmittance. The reflectance values assigned to interior walls, ceiling and floor were 50 %, 80 % and 20 %, respectively. A PS with an 80 % reflectance, 3 mm thickness and 84 rectangular holes accounting for a 40 % perforation ratio is used as an example of complex geometry. First, the PS is placed at a distance of 60 cm from the glazing, as Figure 1 shows. Then, the PS is moved at 10 cm from the glazing to test the influence of varying this parameter.

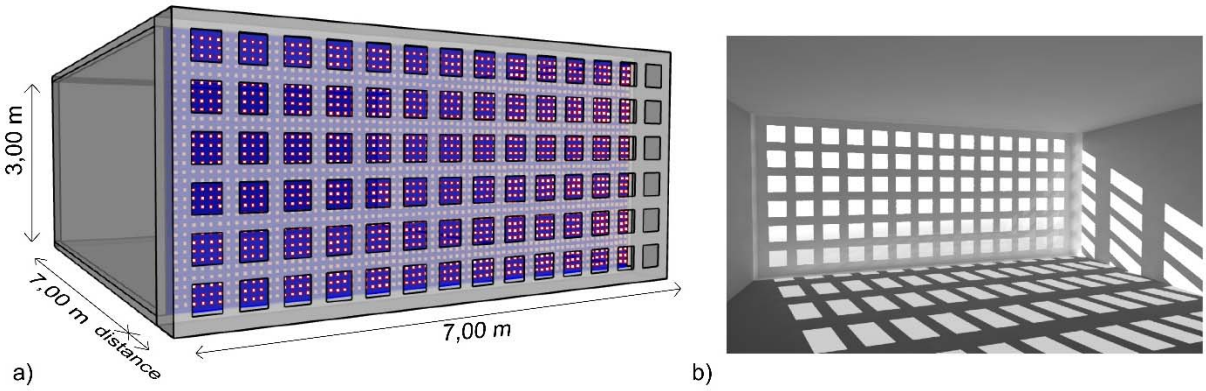


**Figure 1 – a) Perspective view of the case study. The vertical plane used to place the virtual sensors for the solar irradiation simulation is visible behind the PS. b) Rendering of the case study with sky conditions generated from the Seville climate file with the Perez All-Weather model for the 22nd December at 12:00 h.**

Since EnergyPlus is not able to model the PS geometry accurately, the following strategies were adopted for its analysis. First, Rhinoceros was used to model the PS geometry with a perforated mesh exactly as it was set above. Then, Radiance was used to calculate the solar irradiation falling on a vertical plane placed 5 cm from the glazing, for each daylit hour in a year. A sensor grid with a spacing of 10 cm was created on the plane. After performing a convergence test, the following ambient parameters were used for the 2PH method: –ab 5 –ad 44 800. Two irradiance simulations were run for each case: one without the PS, and one with the PS in place. For both calculations, all interior walls, ceiling and floor were assumed to be black surfaces with a zero reflectance value, to exclude all inter-reflections coming from the interior surfaces. From the resulting irradiance profiles, hourly SC were generated by calculating the ratio of the solar irradiation with solar protection in place to that without solar protection. The resulting transparency schedules were then imported in EnergyPlus to run the energy simulation.

A second simplified modelling strategy was followed by replacing the PS geometry with a rectangular planar surface that was modelled with a 40 % fixed annual transmittance in EnergyPlus. Additionally, a BSDF was generated from the geometry of the PS-glazing system and surface properties of its materials, using the Radiance genBSDF command. The BSDF was used in this work to characterize the angularly resolved transmission and reflection of light through the PS. Then, the BSDF data was used in daylight calculations to compare the resulting illuminances against those from the previous strategies. In all simulations, the weather file used was the EPW for Seville, Spain.

## 2.2 Radiance and EnergyPlus simulation

The Radiance technique used to calculate the solar irradiation was the 2-phase method (2PH) with an MF: 6 sky subdivision. The 2PH assigns the sun luminance to three sky patches surrounding the actual sun position and the sky subdivision can have variable resolution by subdividing each patch in smaller parts. The sun and sky contributions can therefore be accounted for in a single run and the computation load can noticeably diminish. Everything is stochastically sampled and the sun is defined with a glow material like the rest of the sky. However, the suggested ambient parameters are therefore switching off any interpolation and ambient catching (i.e. –aa 0, –ar 0).

In this work, the 2PH allowed considering not only the total irradiance passing through the PS but also the irradiance values of inter-reflections within the PS-glazing system. Thus, an hourly profile of indirect irradiation for the whole year can also be generated to analyse when the inter-reflections happen more often. Furthermore, the indirect irradiance contribution can be weighted in annual energy consumption.

The 2PH was also implemented to calculate the Total Annual Illumination (TAI) as the sum of all the illuminance values for the occupied hours in a year. This cumulative metric was chosen since it is more directly affected by differences in methodology, while CBDM metrics tend to smooth those differences by binning absolute values in percentages. The three energy modelling strategies were also considered for daylight simulations to analyse their impact on illuminance results. For all cases, the TAI was calculated on a working plane 80 cm above the floor and 50 cm from the room perimeter. The occupancy schedule was 8 h to 18 h, from Monday to Friday, considering daylight saving time.

After calculating illuminances over the working plane, three specific lighting schedules were generated to model electric lighting use based on a simple on/off switch model, assuming that electric lights are on whenever the room is occupied and the average horizontal illuminance is below 300 lx. The lighting power density was 17,6 W/m$^2$. Every resulting file was an input for the artificial lighting energy calculation of its corresponding modelling strategy in EnergyPlus.

The energy calculations were conducted in Archsim, an interface than links EnergyPlus simulation engine with a CAD modelling environment and a powerful parametric design tool (Rhinoceros and Grasshopper, respectively). For the first simplification case, the hourly SC generated from the irradiation calculations were coupled with the thermal analysis by using an annual transparency schedule. For the second case, a simple rectangle with a 40 % transmittance for all hours of the year was used instead of the complex geometry.

For thermal dynamic simulations, the interior walls, ceiling and floor of the case study were set to be adiabatic; only the fully glazed façade was exposed to the outdoor environment. The glazing system consisted of a clear double-glazing (6 mm), separated by a 13 mm air gap, with a U-value of 2,785 W/m$^2$-K and SGHC of 0,703. In order to focus on studying the performance of the tested PS, the HVAC modelling of a specific system was avoided by selecting the EnergyPlus software option of ‘An ideal Loads Air System’. The occupancy and equipment loads were 1 people/m$^2$ and 12 W/m$^2$, respectively.

## 2.3 Statistical analysis

To analyse the variability of transmitted solar radiation, global and indirect irradiances were plotted as temporal maps. Thus, the inter-reflections between the inner face of the PS and the glazing could be quantified. In addition, the influence of varying the distance within the PS-glazing system on the inter-reflections throughout the year was also analysed. The final aim

was to test whether it is necessary to calculate SC for thin screens instead of using a single perforation ratio in the transparency schedules in EnergyPlus.

Furthermore, histograms of the frequency distribution of all the sensors where the global irradiance (direct + inter-reflected) was recorded, were constructed. All data were grouped in bins to estimate the proportion of cases that fall into specific ranges of global irradiances that primarily represent shadowed or lighted areas. To further illustrate the difference in the distribution of global irradiances during summer and winter, specific instances were chosen: June 22$^{nd}$ and December 22$^{nd}$, both at several hours during the day. For these two instances, the simulations were run under a CIE clear sky model, in order to avoid confounding factors due to weather data contained in the EPW climate file and to allow a direct comparison of sunny conditions in summer and winter.

To compare the three different ways of modelling the PS geometry in daylight simulations, combination charts with the TAI results and the lighting use were generated. In addition, tables and graph bars with the total transmitted solar radiation energy and the total annual energy consumption (lighting plus cooling and heating) were generated to analyse the influence of every modelling strategy.

## 3 Discussion and results analysis

### 3.1 Influence of inter-reflections within the PS

The total annual irradiation resulting from the model with the PS at 60 cm from glazing was 489 kWh/m$^2$. In Figure 2a all hourly irradiances are plotted as a temporal map, showing that higher values of global irradiation were achieved during winter, particularly at midday. This result can be attributed to the direct light passing and exiting through holes of the PS due to lower angles between the solar position and the normal of the façade.

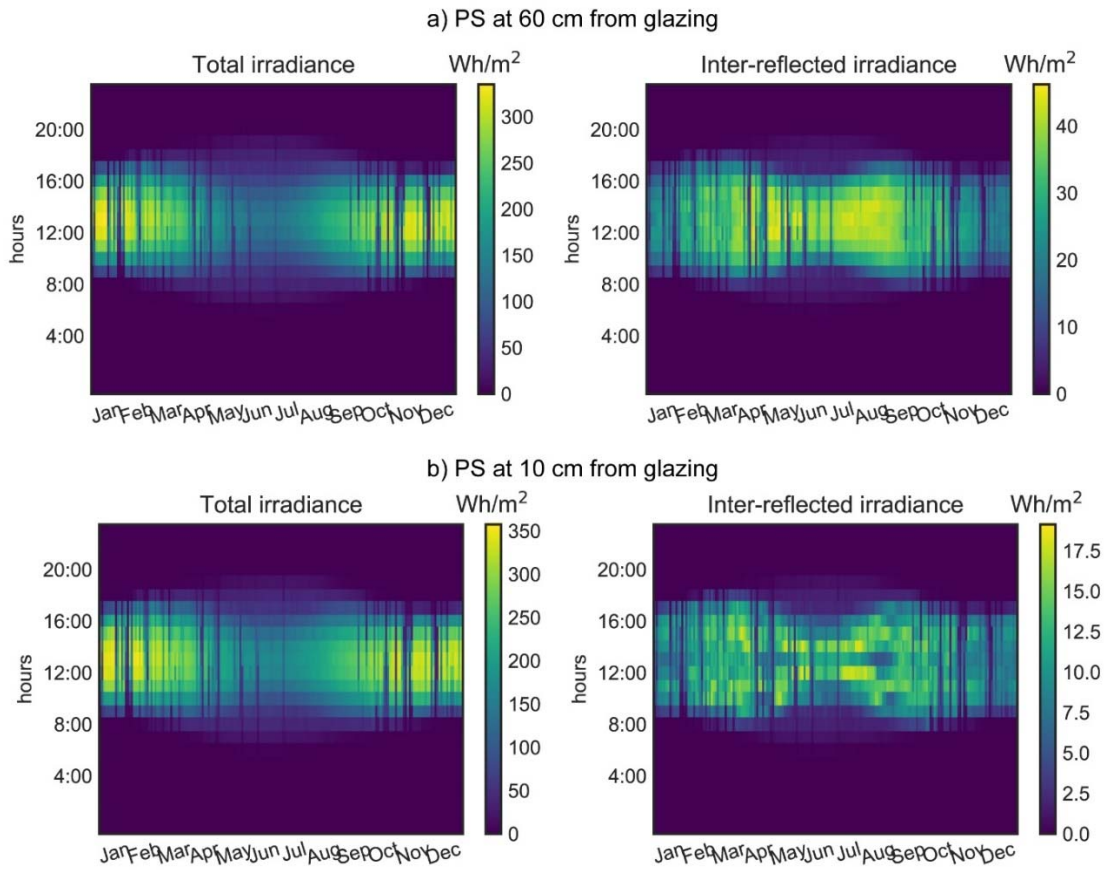


**Figure 2 – Total solar irradiation and irradiation due to inter-reflections within the system, resulting from the model with: a) PS at 60 cm from glazing, and b) PS at 10 cm from glazing. Note that the colorbars scales are different.**

From the total irradiation, 77 kWh/m$^2$ was due to the inter-reflections within the PS-glazing system, accounting for a 16 % contribution. Hence, inter-reflections must not be ignored when analysing the energy performance of PS. As for the previous Figure, all hourly inter-reflections were plotted as a temporal map to understand better the variability of transmitted solar radiation. Figure 2a shows how inter-reflections happen more often during the summer. This is due to sunlight rays passing in between the glazing and the PS plane, and rays being reflected between the two surfaces for higher sun angles.

Regarding the PS at 10 cm from the glazing, the total annual irradiation resulting from the model was 561 kWh/m$^2$. As for the previous, higher values of global irradiation were achieved during winter, as Figure 2b shows. However, the inter-reflected part within the PS-glazing system was 29 kWh/m$^2$, representing only a 5 % contribution. Since the geometry of the PS was the same, the differences from the inter-reflections are attributed to the distance between the PS and glazing. The system characterised by a larger distance between PS and glazing (i.e. 60 cm) resulted in a lower total irradiation value, but the inter-reflections within the system formed a more significant portion of it, whereas the system with 10 cm spacing allowed more solar irradiance to reach the glazing and to enter the space directly, with a reduced contribution from inter-reflections.

To further illustrate the differences in the distribution of global irradiances during summer and winter, specific instances were chosen: June 22$^{nd}$ and December 22$^{nd}$, both at four times during the day. Figure 3 summarizes the results plotted over the vertical grid where the irradiances were calculated. The main differences are attributed to the solar angles and to the distance between PS and glazing. Besides, the histograms in Figure 4 shows a high variability in the global irradiance values. As it can be observed, many sensors were distributed throughout several bins during summer, particularly between 12 h to 16 h. In contrast, a low variability in the global irradiation was observed during winter as most sensors were distributed in a less number of bins. This high variability in the transmitted solar irradiance is due to the large portion of inter-reflections within the system during the summer.

It is clear that the variability of the transmitted solar radiation can be properly accounted by Radiance. Thus, it is expected that the SC will be able to accurately represent this variability throughout the year and to allow the thermal simulation to take it into account. Figure 5 shows the transparency schedules formed from the hourly SC for the PS-glazing system. In addition, Table 1 summarizes the hourly SC obtained for two days and compare its use against the use of a fixed transmittance value for all hours over the year. It can be observed, especially for the PS at 60 cm from the glazing, how a fixed translucent panel cannot represent the variability of transmitted solar radiation, which plays an important role in thermal calculations. Therefore, SC are helpful to enable the performance of solar protection over glazing to be determined. That performance includes not only the direct irradiation but also the indirect component.

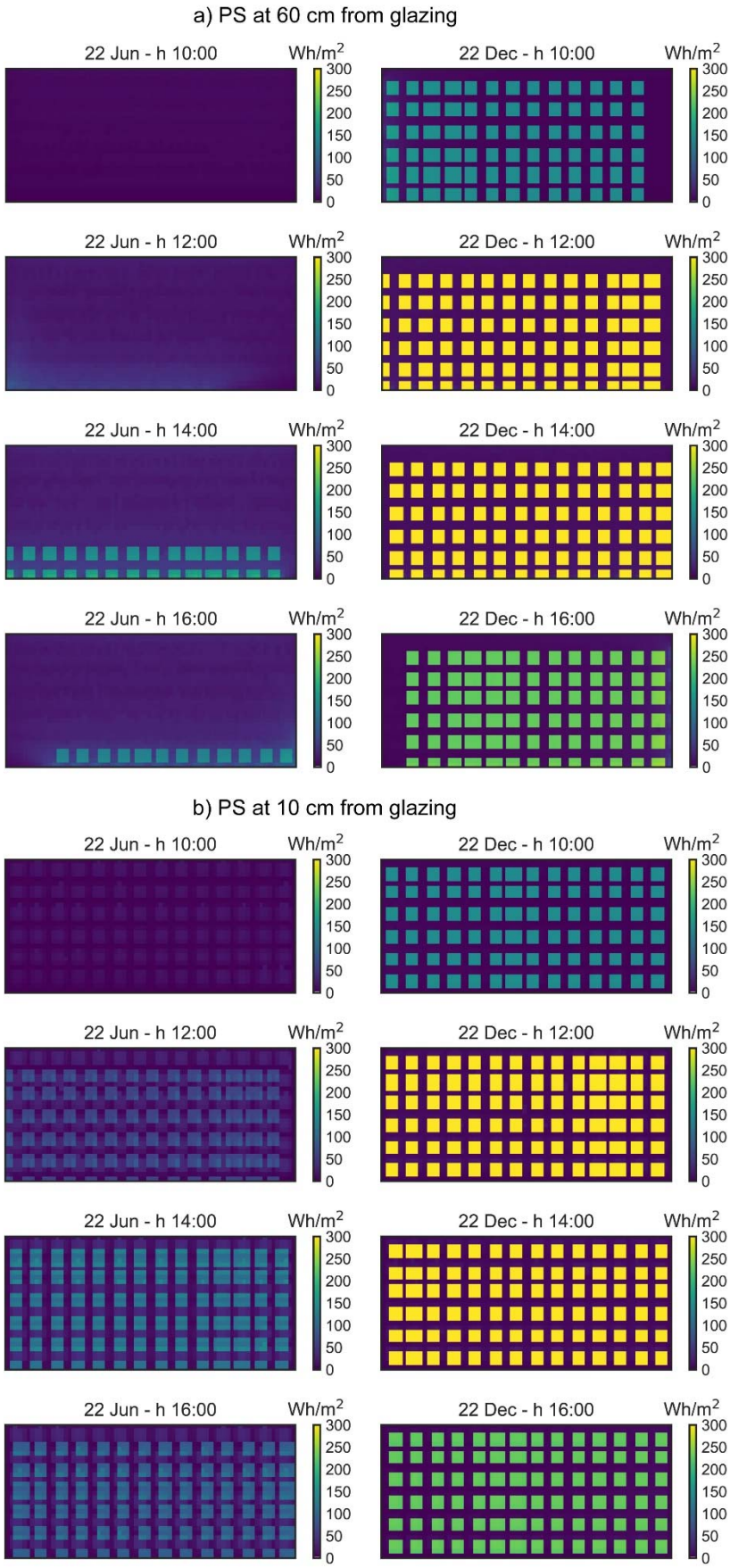


**Figure 3 – Comparison of global irradiances obtained for several instances during two days with clear sky conditions. a) PS at 60 cm from glazing, and b) PS at 10 cm from glazing.**

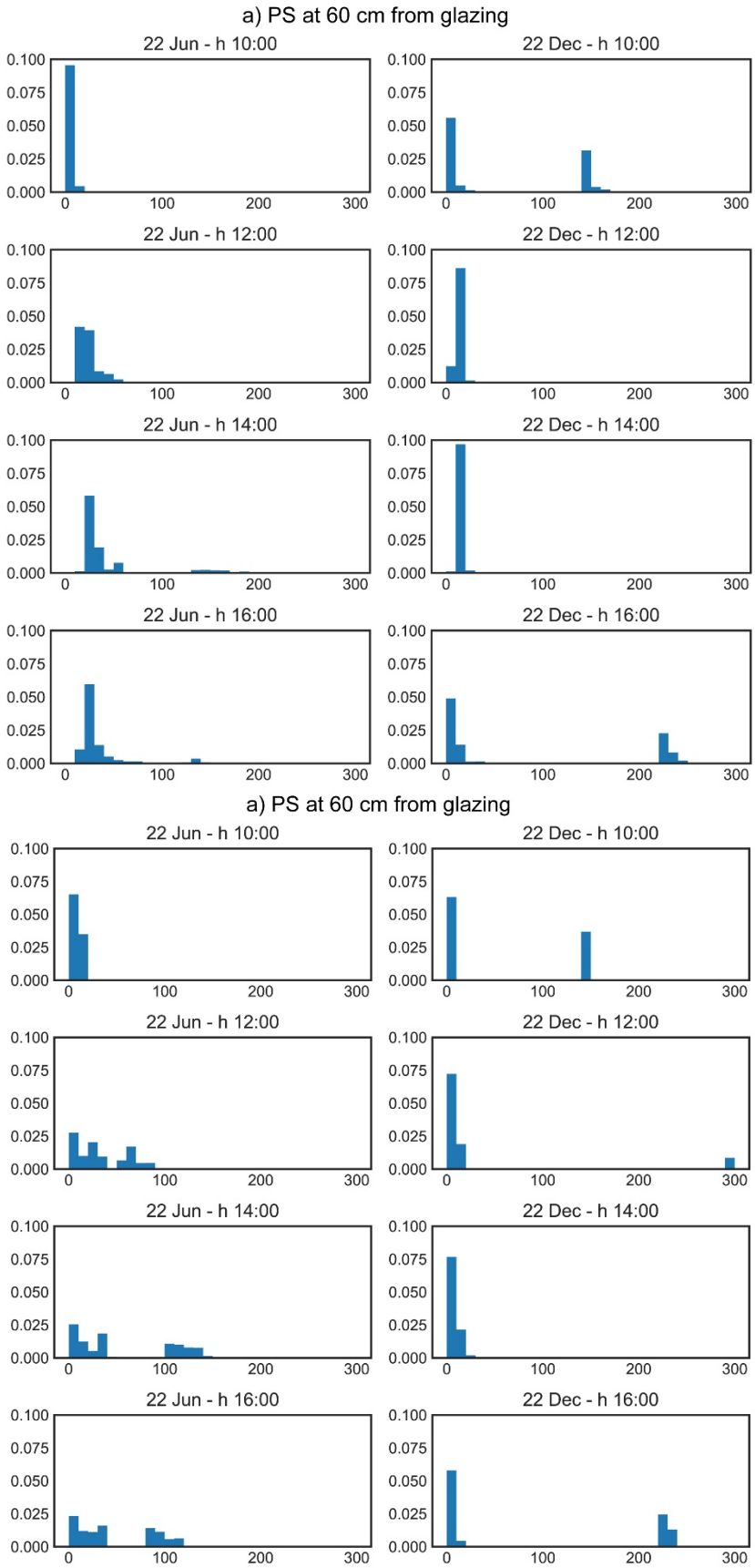


**Figure 4 – Frequency distribution of the total solar irradiation. Results are normalised to show the proportion of sensors over the total, from 0 to 1.**

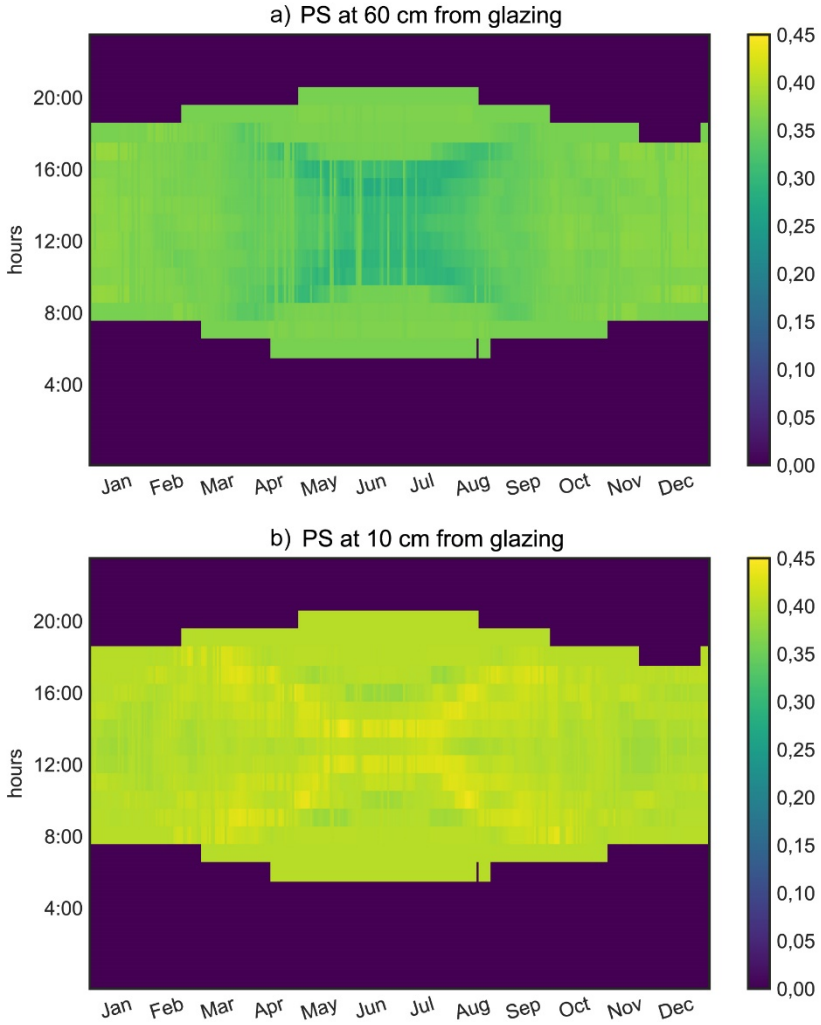


**Figure 5 – Hourly SC forming the transparency schedules for: a) PS at 60 cm from glazing, and b) PS at 10 cm from glazing.**

**Table 1 – Comparison of hourly transparencies (%) used in the energy modelling strategies.**

| | Date/Time | 01 | 02 | 03 | 04 | 05 | 06 | 07 | 08 | 09 | 10 | 11 | 12 | 13 | 14 | 15 | 16 | 17 | 18 | 19 | 20 | 21 | 22 | 23 | 24 |
|---|---|---|---|---|---|---|---|---|---|---|---|---|---|---|---|---|---|---|---|---|---|---|---|---|---|
| JUN | SC_60 | | | | | | | 36 | 36 | 36 | 36 | 30 | 29 | 30 | 30 | 30 | 28 | 31 | 36 | 36 | 36 | 36 | | | |
| | SC_10 | | | | | | | 40 | 40 | 40 | 40 | 38 | 41 | 42 | 40 | 43 | 40 | 38 | 40 | 40 | 40 | 40 | | | |
| | Fixed | 40 | 40 | 40 | 40 | 40 | 40 | 40 | 40 | 40 | 40 | 40 | 40 | 40 | 40 | 40 | 40 | 40 | 40 | 40 | 40 | 40 | 40 | 40 | 40 |
| DEC | SC_60 | | | | | | | | | 36 | 38 | 36 | 37 | 38 | 37 | 38 | 37 | 37 | 38 | | | | | | |
| | SC_10 | | | | | | | | | 40 | 40 | 40 | 40 | 40 | 39 | 40 | 40 | 40 | 41 | | | | | | |
| | Fixed | 40 | 40 | 40 | 40 | 40 | 40 | 40 | 40 | 40 | 40 | 40 | 40 | 40 | 40 | 40 | 40 | 40 | 40 | 40 | 40 | 40 | 40 | 40 | 40 |

## Estimation of TAI and transmitted solar radiation energy

Figure 6 summarizes the TAI results and lighting use. For the first metric, the SC and the BSDF modes, both placed at 60 cm, only achieved a 2 % difference. However, the fixed mode placed at the same distance achieved a reduction of 12 %. These differences were clearly reflected in the number of hours when the light was on.

The total annual energy results are summarized in Table 2. As expected, the transmitted solar radiation energy shows no difference when a fixed transmittance value was used. In contrast, the transparency schedule accounted an 11 % difference between the two distances where the PS was placed. In addition, a 20 % difference was quantified between the SC mode and the fixed one. As for the cooling energy results, a very small difference was achieved between the two distances for the fixed mode, whereas a 6 % difference was accounted between the two

distances for the SC mode. Besides, a 22 % difference was quantified between the two modes. On the other hand, heating energy was little required in the locality under study. Regarding the lighting energy consumption, it was very similar for all PS modes.

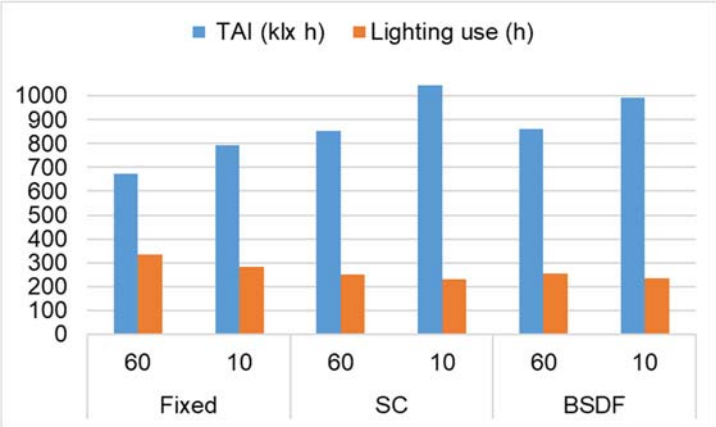


**Figure 6 – TAI results and lighting use for different modelling strategies.**

**Table 2 – Total annual energy results for the three PS modes.**

| PS mode | Distance (cm) | Transmitted solar radiation energy (kWh/m²) | Cooling Energy (kWh/m²) | Heating energy (kWh/m²) | Lighting energy (kWh/m²) |
|---|---|---|---|---|---|
| SC | 60 | 58,76 | 62,15 | 0,35 | 2,68 |
| | 10 | 65,22 | 65,86 | 0,31 | 2,47 |
| Fixed | 60 | 74,08 | 79,41 | 0,32 | 3,03 |
| | 10 | 74,08 | 79,78 | 0,31 | 3,58 |

To understand better the impact of the variability of transmitted solar radiation in cooling energy consumption throughout the year, monthly energy results were summarized in Figure 7. From here, an interrelation between monthly transmitted solar radiation energy and monthly cooling energy consumption was clearly depicted. However, some differences between modes results were observed.

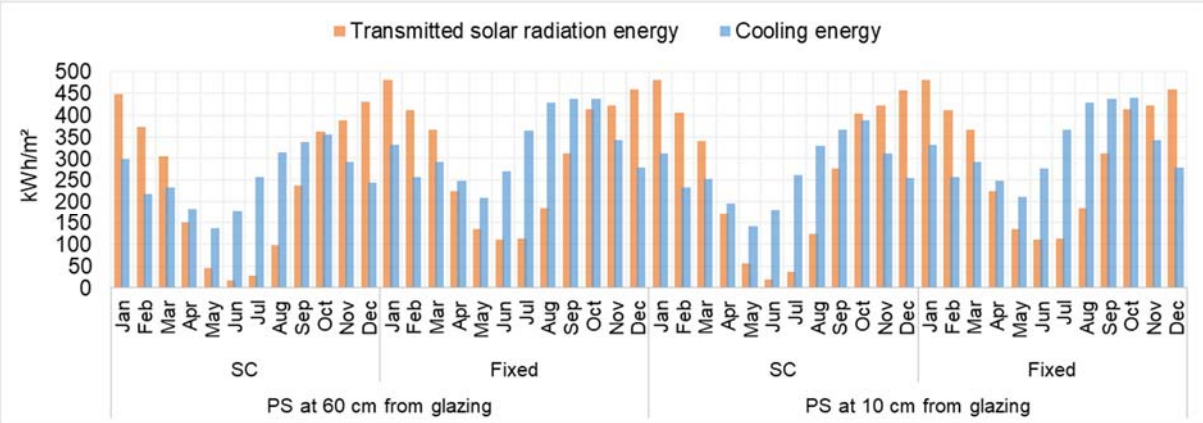


**Figure 7 – Monthly results of the transmitted solar radiation energy and cooling energy. Comparison of using a transparency schedule (SC) and a fixed transmittance value (Fixed).**

Regarding the SC modes, the transmitted solar radiation energy showed a considerable reduction during summer (until 97 % reduction from January to June). Accordingly, the cooling energy demand decreased during those months (64 %). In contrast, the transmitted solar radiation energy increased during autumn and winter due to direct sunlight coming from the South façade. As a result, the cooling energy demand increased during these last seasons.

As regards the fixed modes, the transmitted solar radiation energy accounted smaller differences between summer and winter (until 77 % reduction from January to June) than those accounted in the SC mode. Therefore, the cooling energy consumption had a smaller reduction during summer (52 %). This explains why the total annual cooling energy consumption rose by 22 % when the fixed mode was used in energy calculations.

## 4 Conclusions

This paper investigated and compared different ways of modelling complex shading systems to perform energy simulations in EnergyPlus. Results showed the capability of Radiance to represent properly the variability of transmitted solar radiation through PS by using specific transparency schedules. SC enabled the performance of the system (PS + glazing) to be determined. In short, SC included not only the direct transmitted solar irradiation but also the indirect solar irradiation. In this work, inter-reflections within the system accounted from 5 % to 16 % of the total annual irradiation, so they should not be ignored when analysing the energy performance of PS. It was also found that inter-reflections within the system constituted a larger portion of the total irradiation falling on the glazing when the PS was placed at a larger distance (60 cm in this case).

Additionally, the variability of transmitted solar radiation showed an impact on the total annual energy consumption. For instance, the cooling energy consumption showed a 22 % reduction when using the transparency schedule. These reductions were not adequately considered when using a fixed transmittance value. Therefore, the characterisation of the system through transparency schedules is an important step to carry out when describing the specific behaviour of a thin PS.

The findings here presented are linked to the chosen office and to the PS specific characteristics. However, the approach adopted in this study can be generalised to all applications of transparency schedules in energy simulations, since complex geometries remain a challenging simulation task for EnergyPlus. Hence, future lines of research could further investigate other PS design variables when applying transparency schedules. A wider study currently ongoing is considering a multiplicity of other variables.

## References

Azadeh, O. (2011) ‘Design optimization of a contemporary high performance shading screen – integration of “form” and simulation tools’, in *Proceedings of Building Simulation 2011: 12th Conference of International Building Performance Simulation Association*. Sydney: IBPSA, pp. 2491–2498.

Bellia, L., De Falco, F. and Minichiello, F. (2013) ‘Effects of solar shading devices on energy requirements of standalone office buildings for Italian climates’, *Applied Thermal Engineering*, 54(1), pp. 190–201. (DOI: https://doi.org/10.1016/j.applthermaleng.2013.01.039).

Brembilla, E. *et al.* (2017) ‘Inter-model comparison of five Climate-Based Daylight Modelling techniques : Redirecting glazing / shading systems.’, in *The 15th International Conference of IBPSA*. San Francisco, CA, USA: IBPSA.

Chi, D. A., Moreno, D. and Navarro, J. (2018) ‘Impact of perforated solar screens on daylight availability and low energy use in offices’, *Advances in Building Energy Research*. Taylor & Francis, 0(0), pp. 1–25. (DOI: 10.1080/17512549.2018.1550439).

Kim, D. W. and Park, C. S. (2011) ‘Difficulties and limitations in performance simulation of a double skin façade with EnergyPlus’, *Energy and Buildings*. Elsevier B.V., 43(12), pp. 3635–3645. (DOI: http://dx.doi.org/10.1016/j.enbuild.2011.09.038).

Ramos, G. and Ghisi, E. (2010) ‘Analysis of daylight calculated using the EnergyPlus program’, *Renew Sustain Energy Rev*, 14(7), pp. 1948–1958. (DOI: https://doi.org/10.1016/j.rser.2010.03.040).

Ward, G. (1992) ‘Measuring and modeling anisotropic reflection’, *Computer Graphics*, 26(2), pp. 265–272.